

## Use of Passive Scalar Tagging for the Study of Coherent Structures in the Plane Mixing Layer

By B. R. Ramaprian<sup>1</sup>, N. D. Sandham<sup>2</sup>,  
M. G. Mungal<sup>2</sup> and W. C. Reynolds<sup>2</sup>

Data obtained from the numerical simulation of a two-dimensional mixing layer have been used to study the feasibility of using the instantaneous concentration of a passive scalar for detecting the typical coherent structures in the flow. The study has shown that this technique works quite satisfactorily and yields results similar to those that can be obtained by using the instantaneous vorticity for structure detection. Using the coherent events deduced by the scalar conditioning technique, the contribution of the coherent events to the total turbulent momentum and scalar transport has been estimated. It is found that the contribution from the typical coherent events is of the same order as that of the time-mean value. However, the individual contributions become very large during the pairing of these structures. The increase is particularly spectacular in the case of the Reynolds shear stress.

### 1. Introduction

Several techniques have been used in the past to deduce and study organized structures in turbulent shear flows. These vary from simple level detection of the velocity signal to the use of various types of short-time averages of the flow properties. A relatively simple technique which proved to be very successful in a recent study of the two-dimensional wake of a flat plate (Jovic and Ramaprian [1986]) consisted of using heat as a passive scalar to tag the flow. In this experiment one side of the wake was maintained at a uniformly higher temperature relative to the other side. The resulting instantaneous temperature levels in the flow were found to provide a convenient and simple means of detecting the arrival of organized structures at the probe. In fact, with this technique, it was possible to isolate and study organized structures in the flow even at distances of the order of 250 momentum thicknesses downstream of the trailing edge using only single point measurements. The results of this study are in good agreement with the recent findings of other researchers (Browne *et al.* [1986], Hussain and Hayakawa [1987]) who have used more sophisticated techniques for the eduction and analysis of the organized structures.

The success of the heat tagging technique in detecting organized large-scale structures suggests that there is a strong correlation between passive scalar transport and the large scale structure and that presumably the former is predominantly brought

<sup>1</sup> Washington State University

<sup>2</sup> Stanford University

about by the latter. It seems also that the manner of introduction of the scalar (uniformly over the entire side of the wake, as opposed to introduction at the trailing edge) contributed to the success of the method. This is apparent from the experiments of Cimbala [1985] in the two-dimensional wake of a cylinder, which clearly showed that the flow field inferred from visualization of the passive scalar depends critically on the location of the point of introduction of the scalar contaminant (and the Schmidt number).

Some of the above issues can be better understood if the scalar tagging technique is tested under conditions when the available flow information is not limited to single-point measurements. It was therefore proposed to apply this technique to study the large scale organized structure of a numerically generated two-dimensional mixing layer, in which case, information on the entire flow field is available at all instants of time. Such a test would enable one not only to determine the power and limitations of the scalar tagging technique as a means of identifying large-scale organized structures but also to understand role of these structures in the process of turbulent transport in the mixing layer. The present paper describes the results of such a numerical study.

## 2. Flow Studied

The flow studied is a two-dimensional mixing layer. The database was produced by Sandham & Reynolds [1987], using a random-walk on the phase of the forcing eigenfunctions to simulate the natural mixing layer. The computations are made for the mixing layer between two streams with scalar concentrations  $G_1 = 1$  ('high scalar' side) and  $G_2 = -1$  ('low scalar' side), and moving at velocities  $U_1 = 2$  and  $U_2 = 1$  respectively. The code is two-dimensional, i.e., the two-dimensional instantaneous Navier-Stokes equations are solved. The computational domain extends from  $x = 0$  to  $x = 200$  initial vorticity thicknesses in the streamwise direction and  $y = -\infty$  to  $y = +\infty$  in the normal direction. The flow development within this domain is computed from the initial time  $t = 0$  to a time corresponding to 640 vorticity time units. At  $x = 0$ , velocity perturbations of a frequency corresponding to the fundamental and subharmonic instability modes of the mixing layer but with a randomly walked phase are introduced. A hyperbolic tangent distribution across the mixing layer is assumed for the scalar. The numerical simulation corresponds to a Reynolds number (based on the initial vorticity thickness) of 100. The simulated mixing layer has been found to agree reasonably well with experimental measurements with respect to growth rate, and distributions of mean velocity and turbulent stresses. Hence, in spite of the rather low Reynolds number and two-dimensionality of the simulation, the numerical data can be considered to be adequate for the purpose of the present studies. In order to avoid the effects of the initial conditions, data corresponding to  $t > 240$  only have been used in the study. Likewise, data corresponding to only two locations, namely  $x = 78$  and  $x = 137$  have been used in the present study. These locations are sufficiently far away from the boundaries to be directly influenced by the specified boundary conditions.

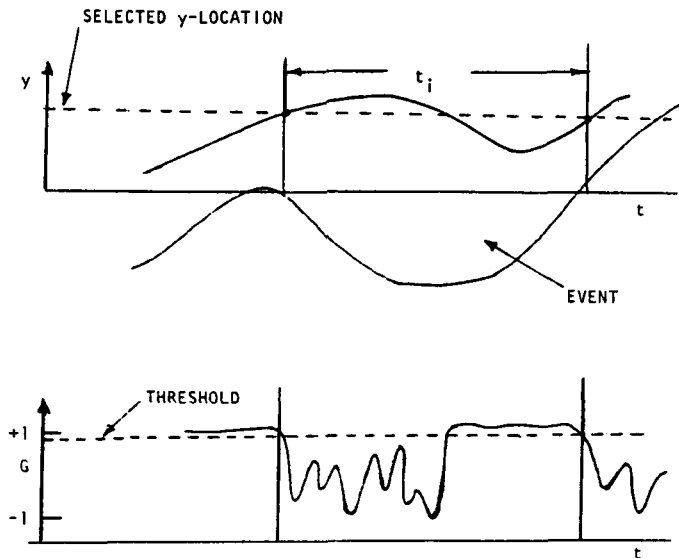


FIGURE 1. Schematic of the eduction procedure

### 3. Eduction Procedure and Results

It was decided to study the organization in the flow in terms of coherent *events* in time rather than coherent *structures* in space. The study thus simulated the experimental situation in which fixed probes measure flow properties as a function of time. Furthermore, averages taken over the events have direct significance since they represent the contribution by the coherent activity to the 'conventional' time-averaged properties. The procedure used for the eduction of the organized structure in the flow was, in principle, similar to that used in the experiments described in Jovic and Ramaprian [1986] and briefly, is as follows. First, a given  $x$ -location is selected for the study. The instantaneous velocity, vorticity and scalar values at this station are each organized in the form of a time series for each  $y$ -location. A  $y$ -location in the 'high scalar' side sufficiently away from the  $y = 0$  line is selected (arbitrarily to begin with). Based on the reasoning that a scalar value of less than 1 at this location indicates contamination with fluid from the 'low scalar' side brought in by the large eddies, the scalar time-series is scanned to detect the time instants when the scalar level crosses a prescribed threshold (say 0.95). The interval between two such crossings from 1 to 0.95 is defined as a large 'event' (see Fig.1). All such events are collected and a histogram of the duration  $t_i$  of these events is generated. Also, the mean duration of the events and the standard deviation are evaluated. The  $y$ -location and the threshold level are optimized so as to minimize the standard deviation of the durations. The resulting normalized histogram is shown in Figure 2 for the station  $x = 78$ , along with the lognormal distribution predicted by Bernal [1988]. The agreement indicates that the random-walk phase model used in the simulation algorithm yields a realistic description of the mixing layer.

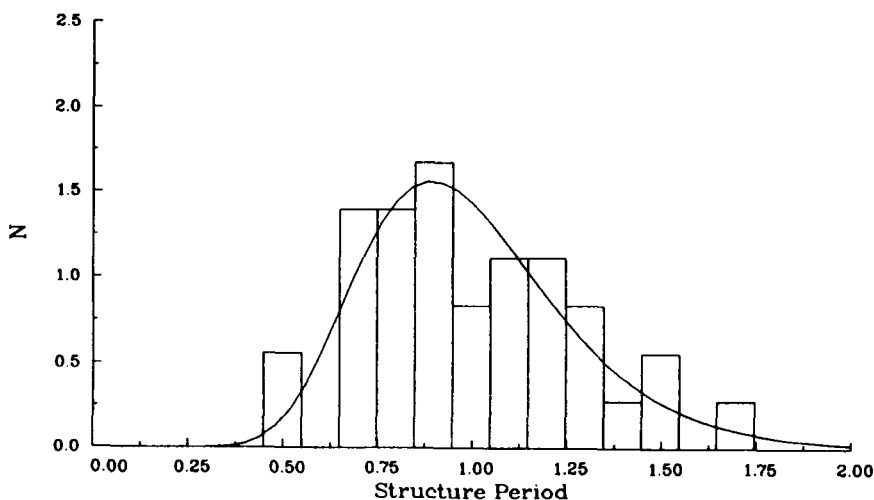


FIGURE 2. Normalized histogram of event durations. Station  $x = 78$ ,  $y = 19$ , scalar threshold=0.95. Mean duration= $10.3 \sigma = 0.315$ . The solid line is the Bernal model.

The next step in the analysis consists of obtaining at all  $y$ -locations, ensemble-averaged values of the velocity components  $U$ ,  $V$ , the vorticity  $\omega$  and the scalar concentration  $G$  at several instants during the event. For this purpose, the time coordinate  $\tau$  is measured relative to the beginning ('front') of the event and is normalized with respect to the duration of the event. Ensemble averages over the several realizations are obtained at ten equally spaced intervals of  $\tau/t_i$ , separately for each duration  $t_i$ . From these ensemble averages, contours of these properties within the event are constructed. Results from this study indicated that not only were realistic contours obtained in each case but also that the contours were nearly the same for *all* the durations in the range  $9 \leq t_i \leq 12$  suggesting thereby that these typical events are indeed coherent. As a final step, the contours are averaged over these different durations to obtain the ensemble-averaged contours for the typical coherent event.

Figures 3 and 4 show typically the results for the scalar concentration  $G$  and the vorticity  $\omega$ . The contours are drawn for equal intervals. These contours are analogous to those that would be obtained in an experiment from the instantaneous outputs of a multitude of probes located across the mixing layer at the given  $x$ -station, as a coherent event passes by the station. The figures clearly show that the scalar conditioning technique has been successful in educing the typical coherent events in the flow. A secondary observation that can be made from the figures is that while details within the event may differ, there is a strong overall correlation between the scalar field and the vorticity field associated with the coherent event. This close correlation perhaps explains why the scalar conditioning technique is successful in educing the coherent (vortical) events in the flow. It is, however,

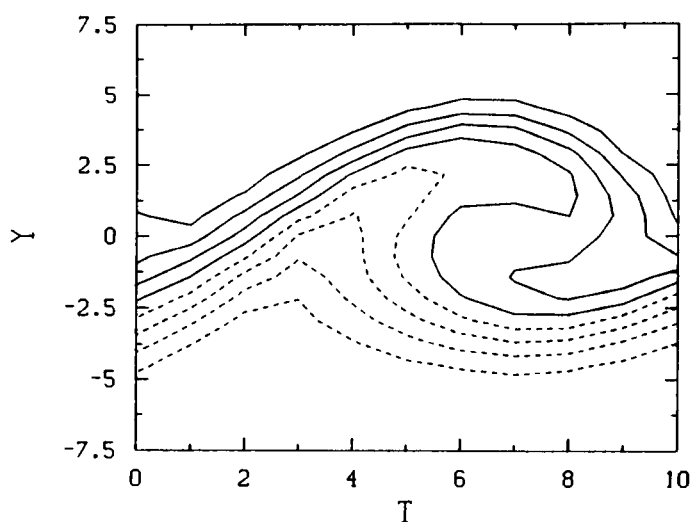


FIGURE 3. Contours of ensemble-averaged scalar concentration in the typical coherent event at station  $x = 78$ .

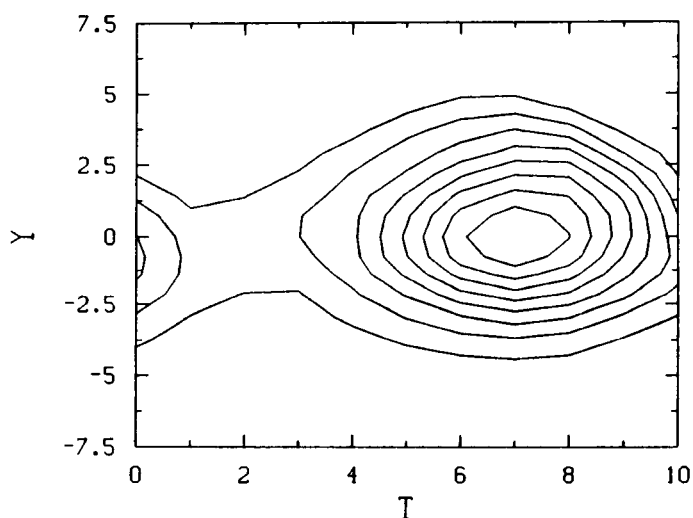


FIGURE 4. Contours of ensemble averaged vorticity in the typical coherent event.

important to note that in this case the Schmidt number of the passive scalar is of the order 1 and that the scalar is 'introduced' at all  $y$ -locations. It is also important to note that there are differences in detail between the scalar and vorticity fields. For example, it is very clearly seen that the scalar gradients are very strong within the braid but there is hardly any spanwise vorticity carried by the braid.

#### 4. Contribution from Coherent Events to Turbulent Transport

The availability of information on the instantaneous flow field in this case, provides an opportunity to study the detailed structure of these typical coherent events and their contribution to the overall turbulent transport. One can estimate, for example, the contribution from the coherent structures to the conventionally defined turbulent shear stress  $\overline{u'v'}$  and the turbulent scalar transport  $\overline{u'g'}$  and  $\overline{v'g'}$  in the streamwise and normal direction respectively. During a coherent event, the instantaneous velocity fluctuations  $u'$  and  $v'$  with respect to the long-time average velocity  $\overline{U}$  and  $\overline{V}$ , and the instantaneous scalar concentration fluctuation  $g'$  with respect to the long-time averaged scalar concentration  $\overline{G}$  can respectively be written as

$$u' = \langle U \rangle + u_s \quad (1)$$

$$v' = \langle V \rangle + v_s \quad (2)$$

$$g' = \langle G \rangle + g_s \quad (3)$$

where the sign  $\langle \rangle$  denotes ensemble-averaged fluctuations with respect to the corresponding long-time average value and the subscript 's' denotes the random departure of the instantaneous value from the ensemble average. The latter can be regarded as 'turbulence' superposed on the deterministic fluctuations. The instantaneous products  $u'v'$ ,  $u'g'$  and  $v'g'$  can then be ensemble averaged for each nondimensional time  $\tau/t_i$  within the typical coherent event and subsequently averaged over the entire duration of the event to obtain

$$\overline{\langle u'v' \rangle} = \overline{\langle U \rangle \langle V \rangle} + \overline{\langle u_s v_s \rangle} \quad (4)$$

$$\overline{\langle u'g' \rangle} = \overline{\langle U \rangle \langle G \rangle} + \overline{\langle u_s g_s \rangle} \quad (5)$$

$$\overline{\langle v'g' \rangle} = \overline{\langle V \rangle \langle G \rangle} + \overline{\langle v_s g_s \rangle} \quad (6)$$

The left hand side of the above equations represent the contribution from a typical coherent event to the time-average transport. The two terms on the right hand side represent the contributions respectively from the deterministic and the random part of the fluctuations associated with this typical event.

Typical results for the station  $x = 78$  are shown in Figs. 5 and 6 for the shear stress and the scalar transport in the normal direction respectively. It is seen that the superposed turbulence (which can be regarded as representing the jitter associated with the process of ensemble averaging) is as large as the organized component in the case of the shear stress but is less significant in the case of the scalar flux. However, at  $x = 137$ , the level of the superposed shear stress also was found to have a relatively small magnitude. In any case, the *total* contribution from the typical coherent event, given by the sum of the two components is seen to be about 60 % of the time-mean value. Similarly, at  $x = 137$  this contribution was found to be approximately equal in magnitude to the time-mean value. Figure 10 shows similar results for the scalar transport. Results for the streamwise scalar transport also showed a similar trend. It is thus concluded that the typical coherent

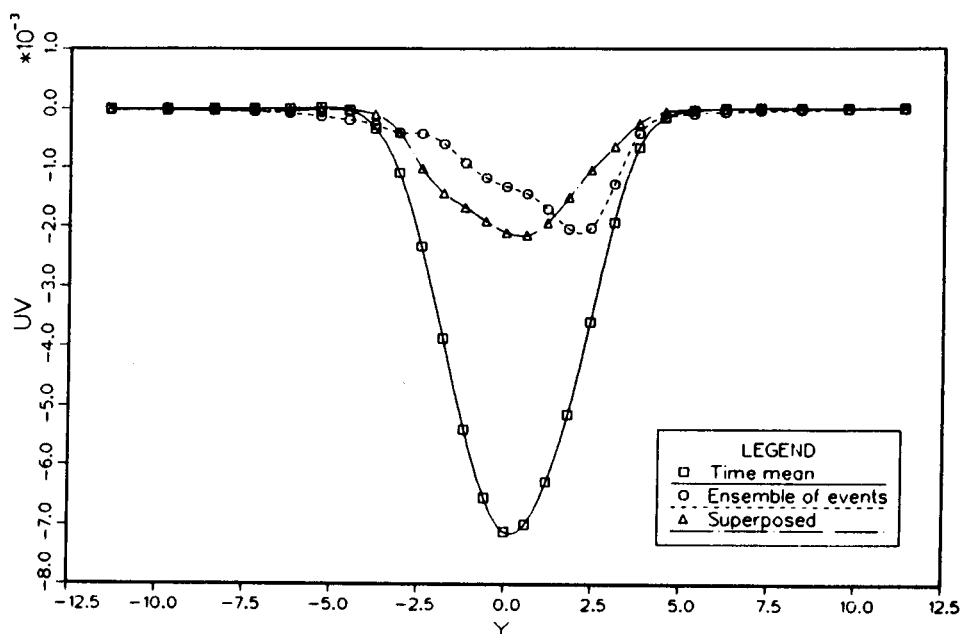


FIGURE 5. Contribution from the typical coherent event to turbulent shear stress. Station  $x = 137$ .

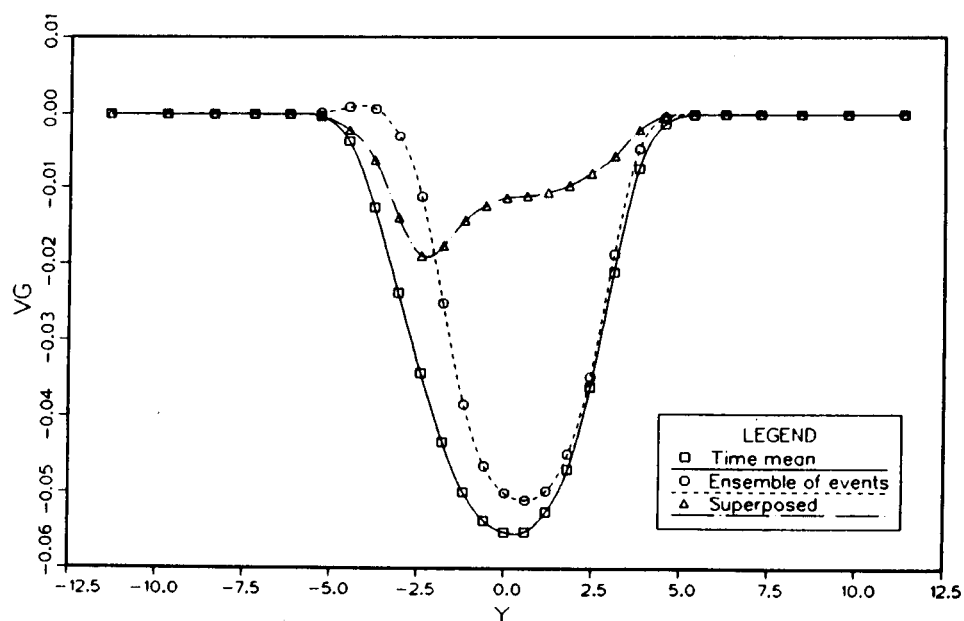


FIGURE 6. Contribution from the typical coherent event to turbulent transport of scalar in the normal direction. Station  $x = 137$ .

events carry shear stress and heat flux of approximately similar magnitude as the corresponding time-mean values. Hence, these typical coherent events are perhaps as significant as the rest of the events in the flow (but not necessarily the most significant) from the point of view of turbulent transport. The result, however, differs from the experimental results for the wake obtained in Jovic and Ramaprian [1986] which indicated that the shear stress associated with the coherent motion was 2 to 3 times larger than the time-mean value. This difference in the results must be due to the fundamental differences between the dynamics of the mixing layer and the far-wake, though effects of three-dimensionality and contamination with atypical events during eduction in the experiments might have contributed somewhat to the observed differences.

## 5. Results for a Pairing Event

The above results correspond to the so called typical coherent event observed at a given  $x$ -location. The mixing layer, however, is characterized by pairings of the coherent structures, which occur at random streamwise locations. However, it is likely that at any  $x$ -location, a pairing event can be observed if one waits for a long enough time. The rather restricted space-time domain of the present numerical simulation did not allow a large enough number of such pairing events to be sampled and ensemble averaged. However, individual pairing events were isolated and studied. The results for one such event, corresponding to the completion of a pairing at  $x=137$  are discussed here. The results shown are expected to be typical of this phase of the pairing process.

Figures 7 and 8 show the scalar concentration and vorticity contours for the pairing event. Once again, overall topological similarity can be observed between the scalar and vorticity fields. However, the scalar gradients in the interior of the event are less strong than those of vorticity, which shows a nearly uniform variation from the center to the outer edge of the structure. Figures 9 and 10 show the cross-stream distribution of the transport terms for momentum and scalar. The same nomenclature as was used in Fig.5 and 6 has been retained even though the ensemble 'average' has been obtained over only *one* realization and hence the superposed component is zero. It is seen that the organized motion associated with the pairing event carries nearly eight times the value of the time-mean maximum shear stress in the mixing layer. On the other hand, the contribution from the pairing event to the scalar transport is of the same order as the time-mean value. Comparing these results with those for the typical coherent event, one can conclude that pairing events are responsible for bringing about a significant amount of turbulent transport. The contribution to transport of momentum is indeed spectacular during pairing, while the contribution to scalar transport is only moderate. Browand & Weidman [1976] have shown experimentally that single events lead to Reynolds stresses that are comparable to the time average, while pairing events are very significant with respect to Reynolds stress production; results that are consistent with our findings. The results shown in Figs. 9 and 10 may be slightly modified if ensemble averages are obtained over a large number of realizations. However, the events are so strongly



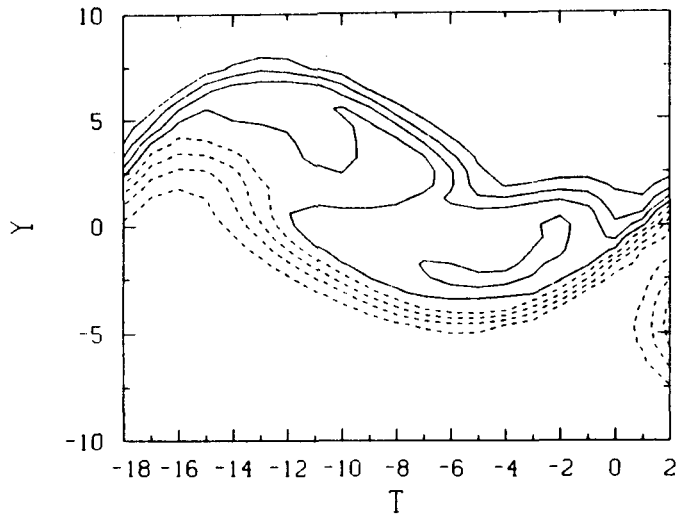


FIGURE 7. Contours of scalar concentration for a pairing event. Station  $x = 137$ .

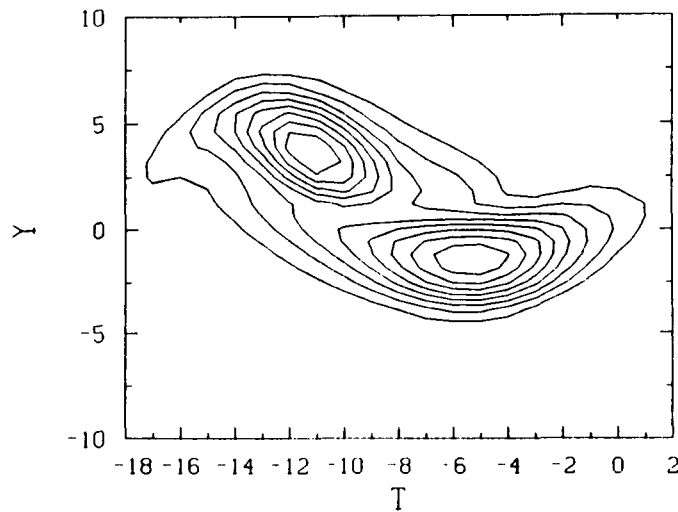


FIGURE 8. Contours of vorticity for a pairing event. Station  $x = 137$ .

coherent that it is unlikely that a major departure from this trend would emerge from the study of a large number of realizations.

## 6. Comparison of Scalar Conditioning with Vorticity Conditioning

Finally, it is instructive to compare the present eduction technique based on scalar level conditioning with other techniques. Unfortunately, it was not possible to make extensive comparisons with several techniques due to time-constraint. However, comparisons of the present results were made with those obtained using vorticity

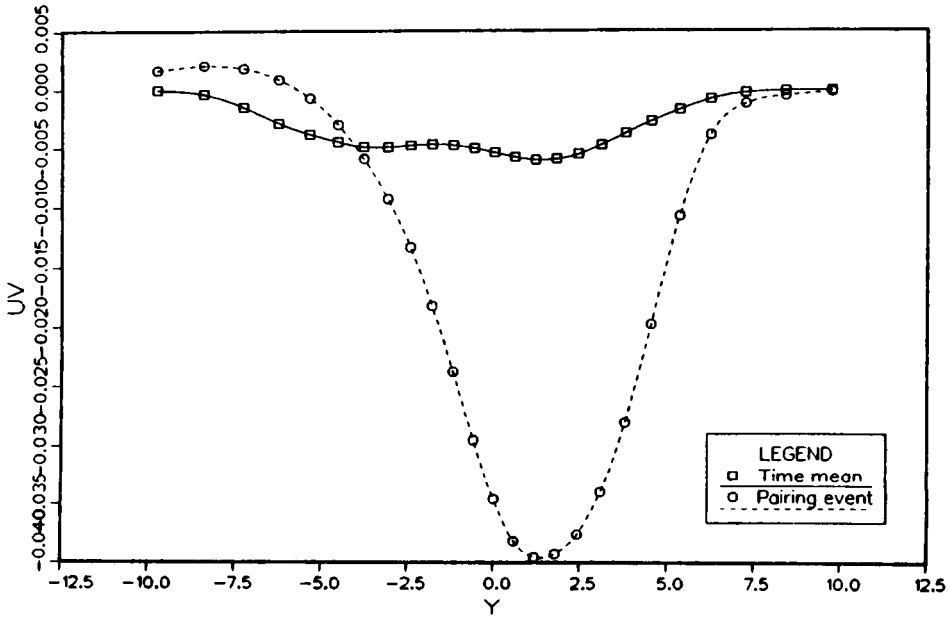


FIGURE 9. Contribution from the pairing event to the turbulent shear stress. Station  $x = 137$

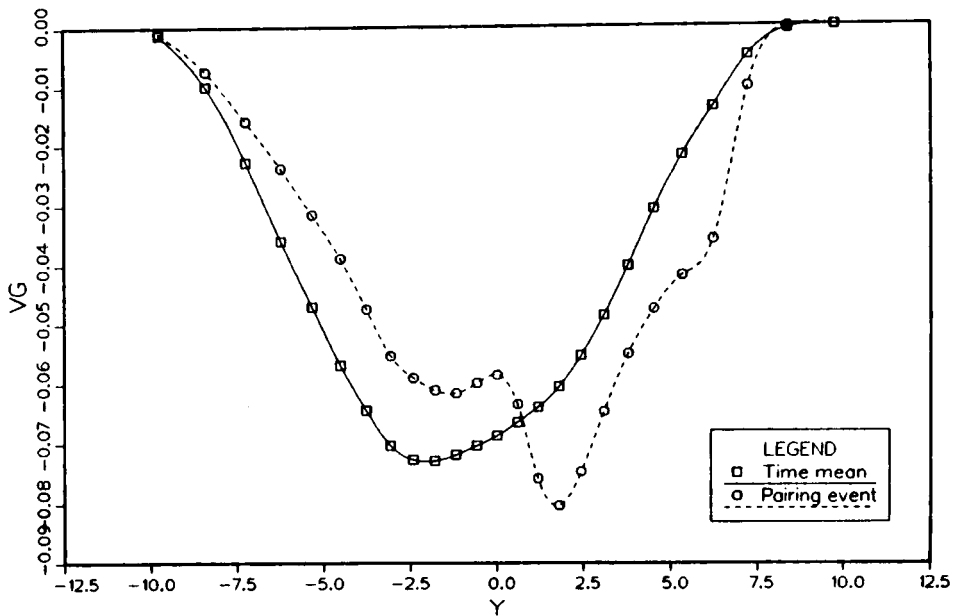


FIGURE 10. Contribution from the pairing event to the turbulent transport of the scalar in the normal direction. Station  $x = 137$

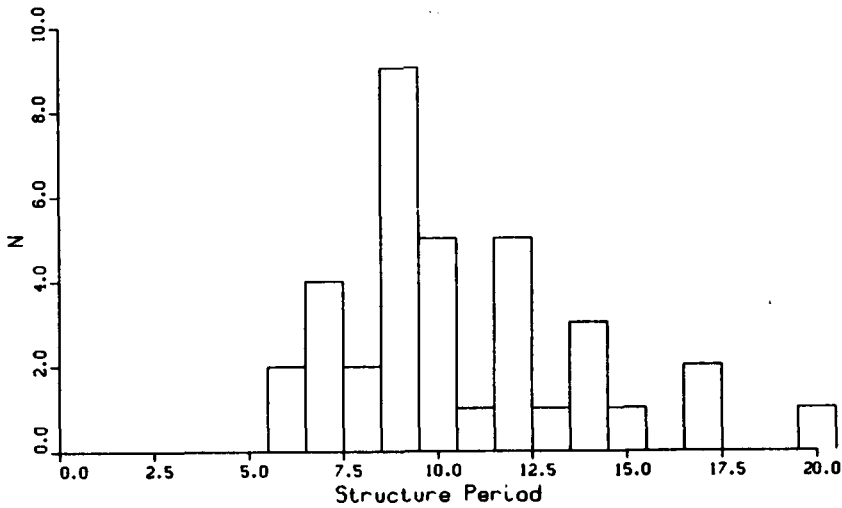


FIGURE 11. Histogram of event durations. Station  $x = 78$ ,  $y = 19$ , vorticity threshold=0.04. Mean duration of events=10.6,  $\sigma = 0.31$

level for the eduction of the coherent events. Vorticity is often regarded as the best criterion for the identification of the coherent structures. Instantaneous vorticity is, however, one of the most difficult quantities to monitor in an experiment. In the present numerically simulated mixing layer, however, instantaneous vorticity values were readily available. The eduction procedure used was analogous to that used with the scalar. Thus, a suitable  $y$ -location and a vorticity threshold level are selected by trial and error. Crossings of this level by the vorticity values in the increasing direction from zero are assumed to be associated with the passage of the coherent (vortical) events. Optimized histogram and ensemble averages are then obtained as in the case of scalar conditioning. Figure 11 shows the histogram of the duration of the coherent events. This can be compared with Figure 2. It is seen that while there are some differences in detail, the two histograms are quite similar. The mean duration of the events was nearly the same in the two cases. So also are the durations of the most frequent events. In fact, the contours of ensemble averaged scalar concentration and vorticity were found to be indistinguishable from those shown in Figs. 2 and 3 and are not therefore presented separately. The contours of ensemble-averaged shear stress  $\langle U \rangle \langle V \rangle$  (corresponding to the organized motion) obtained with the two techniques are compared in Fig.12. It is seen that there are only very small differences between the two results. For example, there is only a 4% difference in the maximum values (and also minimum values) for the two cases. A somewhat larger difference (about 15%) was found in the value of the total shear stress carried by the coherent event. Even this difference is well within the uncertainties to be expected in a study such as this, especially when a small number of realizations are used to obtain the ensemble averages. It appears reasonable to conclude that with scalar tagging and conditioning, it is possible to

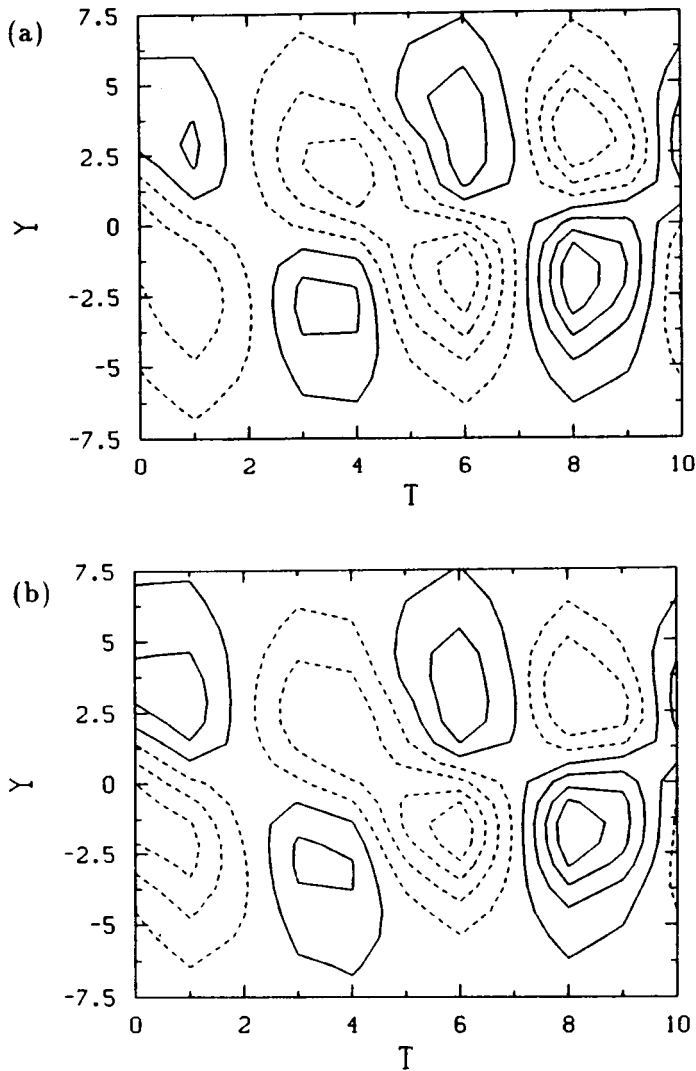


FIGURE 12. Contours of the ensemble-averaged shear stress  $\langle U \rangle \langle V \rangle$  in the typical coherent event. Station  $x = 78$ . (a) from scalar conditioning (b) from vorticity conditioning.

isolate the typical coherent structures as reliably as with the more difficult vorticity conditioning technique.

## 7. Concluding Remarks

The present study, though limited in scope by time constraints, has led to some interesting observations and useful results. The study has demonstrated that, if properly used, passive scalar conditioning can prove to be a simple and effective

technique for the eduction and analysis of large-scale coherent structures in turbulent shear flows. The reason for its success is the fact that the scalar field under such conditions closely resembles the vortical field in respect of overall features like topology and large-scale structure. There are however differences between the two fields in respect of finer details within the structure. But, these latter differences do not affect the eduction process significantly. In fact, eduction based on scalar conditioning captures more or less the *same* structures as those captured by an alternate technique such as vorticity conditioning. The key requirements for the success of the scalar conditioning technique, however, are that the *entire stream* on one side of the mixing layer is maintained at a uniform scalar concentration and that the Schmidt number of the scalar is close to unity.

The study of the ensemble averaged properties associated with the coherent events was also very useful, in spite of the several restrictive test conditions, such as the use of two-dimensional simulation, low Reynolds number, arbitrary (though reasonable) initial forcing and downstream boundary conditions, and the small number of realizations under which it was conducted. This study showed that typical coherent events carry a significant amount of 'turbulence' and can therefore affect the overall transport of momentum and scalar in a significant manner. However, even more significant are the pairing events in affecting these transport phenomena. Particularly spectacular is the role of these events in the transport of momentum, which reaches several times the time-mean value. Scalar transport is not significantly increased during these events.

## REFERENCES

- JOVIC, S. AND RAMAPRIAN, B.R. IIHR Report 298, University of Iowa, Iowa City (1986).
- BROWNE, L.W.B., ANTONIA, R.A. AND BISSET, D.K. 1986 . *Phys. Fluids*. **29**, 3612.
- HUSSAIN, A.K.M.F. AND HAYAKAWA, M.J. 1987 . *J. Fluid Mech.* **180**, 193.
- CIMBALA, J.M., NAGIB, H. M. AND ROSHKO, A. 1988 . *J. Fluid Mech.* **190**, 295-298.
- SANDHAM, N.D. AND REYNOLDS, W.C. Proceedings of the Sixth Symposium on Turbulent Shear Flows , Toulouse, France. (1987).
- BERNAL, L.P. 1988 . *Phys. Fluids*. **31**, (4), Sept. 1988, 2533.
- BROWAND, F.K. & WEIDMAN, P.D. 1976 . *J. Fluid Mech.* **76**, 127-144.